CrossMark

ORIGINAL RESEARCH PAPER

Identification of the nonlinear seismic response of buildings by a combined Stockwell Transform and deconvolution interferometry approach

Giovanna Pianese[1] · Bojana Petrovic[2] · Stefano Parolai[2] ·
Roberto Paolucci[1]

Abstract In presence of soil–structure interaction (SSI), changes in dynamic properties of the system can be related to nonlinearities in both the structural and soil response. Identifying the nonlinearities related to non-stationary phenomena due to structural damage is an important issue for damage detection and localization. In this study, a novel approach is proposed to identify the non-linear structural response of an instrumented building in presence of SSI. Considering the advantages provided by the use of the time–frequency representation to explore the time-variant behavior of the system, and the direct evaluation of the shear wave velocity by the use of the deconvolution interferometry to decouple structural response from soil response, a combined Stockwell Transform and deconvolution interferometry approach is presented. The combined approach is applied to a selected data set of a well-documented building, the Jalapa building, whose nonlinear response was already investigated with other methods. This offers the possibility to validate the results obtained by the proposed approach. Jalapa building is a reinforced concrete structure, located on soft clay in Mexico City. Both SSI effects and structural and nonstructural damage affected the building response during earthquakes in the 1990s. The building was retrofitted twice during its lifetime. The data of three events are considered when investigating the changes in dynamic properties of the structure due to damage and retrofitting. The results allow us to detect the different phases of non-linear structural response in a reasonable agreement with the documented status of the building after each event.

Keywords Nonlinear response · Stockwell Transform · Deconvolution interferometry · Structural damage · Soil–structure interaction

✉ Giovanna Pianese
giovanna.pianese@polimi.it

1 Department of Civil and Environmental Engineering, Politecnico di Milano, Piazza Leonardo da Vinci 32, 20133 Milan, Italy

2 Helmholtz Centre Potsdam, GFZ German Research Centre for Geosciences, Potsdam, Germany

 Springer

1 Introduction

The need of effective knowledge of the status of ageing structures has increased markedly the interest in the development of structural monitoring techniques with the aim of identifying possible earthquake related damage. For this purpose, usually the changes in dynamic parameters (e.g., elastic moduli, shear wave velocity, fundamental frequency) during an earthquake are monitored. It is considered the simplest way to detect the onset of structural damage and its impact on the dynamic response of the building. Moreover, in presence of soil–structure interaction, the fundamental frequency of the system, and hence its variation, estimated from seismic data recorded in the building, can give a misleading evaluation of the dynamic properties of the structure. This is due to the fact that detected variations of the frequencies may be related as well to nonlinearities in the foundation, the structural elements, or both (e.g. Trifunac et al. 2008; Michel et al. 2011; Rahmani et al. 2015). For monitoring the status of a building, it is necessary to separate the response of the building from soil–structure coupling.

In recent years, monitoring the status of buildings by installing sensors in different positions in the building and processing the recorded motions has been made easier by the rapid development of low-cost instruments and the increased capacity for data acquisition and transmission. Assessing damage evolution through monitoring the structural response allows one to better understand the dynamic behavior of structures. Since only a limited number of moderate to strong earthquakes occurs close to well-instrumented buildings, the nonlinear dynamic behavior is usually studied through numerical analysis. This kind of analysis presents several drawbacks, like simplified modelling assumptions, and the difficulty in the proper calibration of mechanical parameters for damaged structures and materials.

Regarding methods based on empirical data, the seismic response of a system is classically determined by estimating the characteristics of the normal modes by using the vibrational approach (e.g., Chopra 1996). Moreover information on the building's properties are obtained by studying seismic waves through the building by the waveform approach (e.g., Kanai 1965; Safak 1989; Snieder and Safak 2006; Kohler et al. 2005, 2007; Prieto et al. 2010; Todorovska 2009b; Rahmani and Todorovska 2013; Bindi et al. 2014; Wen and Kalkan 2017).

Starting from the idea of Kanai (1965), the dynamic behavior is studied via wave propagation through the building by analyzing the shear wave velocity, which is a function of the structural material. The main advantage of deconvolution interferometry (when the station at roof is used as reference) is that it allows one to retrieve the structural response, irrespective of the amount of coupling with soil, manifested by soil–structure effects (e.g. Snieder and Safak 2006; Todorovska 2009a, b; Michel et al. 2011).

Both vibrational and waveform approach are not reliable when the dynamic response evolves over time because of the loss of information about the local spectrum and the time-varying behavior.

Several techniques for signal analysis and identification of structural dynamics have been proposed in the past with the aim to evaluate the dynamic characteristic of a soil–structure system over time. The time–frequency techniques (e.g., Gabor 1946; Cohen 1989; Stockwell et al. 1996; Mallat 1998; Addison 2002; Bradford et al. 2006; Dehghani 2009), introduced for the time–frequency analysis of geophysical signals, have led to significant advances in monitoring nonlinear behavior of buildings (e.g., Mucciarelli et al. 2004; Michel and Guéguen 2010; Puglia et al. 2011; Ditommaso et al. 2012). Moreover, the time–frequency analysis has been applied on seismic data recorded in buildings in presence

of SSI, in order to examine possible time-variations of the soil–structure system frequency during an earthquake (e.g., Trifunac et al. 2001; Todorovska and Trifunac 2007; Rahmani et al. 2015).

Among the different time–frequency techniques, the Stockwell time–frequency representation (S Transform, Stockwell et al. 1996) is considered a powerful time–frequency tool for signal analysis. Compared to the classical techniques for time–frequency analysis (e.g., Gabor 1946; Daubechies 1992; Wigner 1932; Ville 1948; Bradford et al. 2006), this transformation shows a much better resolution and also offers the consideration of a range of fundamental properties, such as linearity and invertibility (e.g., Stockwell et al. 1996; Parolai 2009). The S Transform allows the extraction of the processed information from the signal, without modifying the local spectra characteristics. The amplitudes and phases from the S Transform have a direct link with those of the Fourier transform. Moreover, it is directly invertible back to time domain, allowing a combination of denoising and time–frequency domain filtering (e.g., Pinnegar and Eaton 2003; Schimmel and Gallart 2005; Askari and Siahkoohi 2007; Parolai 2009).

Taking advantage of these properties, the S Transform has been applied to a number of civil engineering purposes, especially for structural health monitoring. Picozzi et al. (2011) applied the S Transform following the 2009 L'Aquila earthquake to study the nonlinear behavior of the Navelli city hall. Ditommaso et al. (2012) proposed a band variable filter based on S Transform to study the characteristic of non-stationary signals. Furthermore, this tool is very useful to isolate the response of individual, time-varying modes of vibration of soil and buildings. Ponzo et al. (2013) applied the band-variable filter to identify and localize damage through the modal curvature variations. However, the latter methodologies were not applied to real data recorded in a damaged building, but are based on numerical analysis (by using synthetic data as inputs) and shaking table tests (subjected to real ground motions) with scaled models.

Moreover, although the waveform approach is based on the linear time-invariant assumption, some authors used this technique, based on deconvolution interferometry (e.g. Kanai 1965) for damage detection (e.g. Ivanovic et al. 2001; Trifunac et al. 2003; Picozzi et al. 2011; Nakata et al. 2013, 2015; Rahmani et al. 2015).

Todorovska and Trifunac (2008a, b) showed that the global changes in structural stiffness can be monitored by analysis of travel time of seismic waves in selected time-windows (windowed deconvolution) and applied the method to real data recorded in two full-scale structures, severely damaged by earthquakes. Picozzi et al. (2011) followed the Todorovska and Trifunac approach and performed the windowed deconvolution to monitor the velocity variation of Navelli City Hall during the second strongest aftershock of the 2009 L'Aquila earthquake.

Recently, Rahmani et al. (2015) presented the time-wave velocity analysis for earthquake damage detection in the buildings. Based on the same conceptual model of Todorovska and Trifunac (2008a, b), the automation of the mowing window analysis and higher accuracy of the identification of travel time of seismic waves have been introduced. Ditommaso and Ponzo (2015) proposed a tool based on windowed deconvolution interferometry and Fourier Transform for the evaluation of the fundamental frequencies of the nonlinear structural response. It was shown that the windowed deconvolution interferometry can be considered a robust method to detect the nonlinear behavior of structures. However, the results are affected by the position and width of the time-windows, where small changes in their position may produce significantly different results (e.g., Rahmani et al. 2015). The accurate calibration of the width of the time-window is essential in order

to minimize the spurious frequency within each impulse response function (e.g. Ditommaso and Ponzo 2015).

Within this context, a novel approach is proposed to detect the nonlinear seismic behavior of a structure in the presence of soil–structure interaction effects. If these effects are not properly accounted for, it may lead to improper evaluation of the dynamic properties of the structure and misinterpretations of their changes during an earthquake. Taking advantage of the mathematical properties of S Transforms (e.g., linearity, a direct link to Fourier Transform), the deconvolution interferometry is applied to each local spectra obtained by the S Transform and the instantaneous impulse response functions (IIRFs) are retrieved. The IIRFs provide an overall picture of the wave propagation through the structure during the seismic event by decoupling the structural response from soil–structure interaction effects. The detection of nonlinear effects is carried out through the estimate of the variations of the shear wave velocity, and hence of the fixed-base frequency of the building (modeled as a shear beam), over time. The changes of dynamic parameters, in case they occur, are reasonably associated with the degradation of the building's structural stiffness over time and can be considered as indicators of the occurrence of damage. The main advantage of the proposed method is that it allows one to follow instant by instant the dynamic response of a structure (decoupled from soil/foundation) automatically due to the nature of Gaussian window in the S Transform (applying the deconvolution interferometry on the local spectra of real data), without previous analysis to calibrate the width and the position of the windows.

The application of the proposed approach deals with earthquake-induced nonlinear response of a structure (the so-called Jalapa building) in presence of soil–structure interaction. The dynamic behavior of Jalapa building was investigated through different approach in the past (e.g., Paolucci 1993; Meli et al. 1998; Cardenas et al. 2000; Murià-Vila et al. 2001; Murià-Vila 2007). It was shown that the dynamic response of the Jalapa building was affected by the nonlinear behavior of the structure, essentially attributed to stiffness changes due to the deterioration of the structural and non-structural element (e.g. Meli et al. 1998; Murià-Vila et al. 2001). Moreover, the dynamic response of Jalapa building changed also due to the retrofitting

For this purpose, the novel approach is applied to recordings of three events in the Jalapa building at different floors under different levels of shaking (two events before retrofitting during which the response of Jalapa building was essentially linear either and nonlinear, and one event recorded after retrofitting during which the dynamic response changed due to damage and retrofitting,) in order to study step-by step the evolution of the dynamic characteristics. The results are presented in terms of instantaneous IIRFs, the evaluation of instantaneous shear wave velocity and finally of fixed-base frequency by assuming the building to behave as a shear beam Finally, the results obtained by novel approach are compared with documented status of the building and with results obtained by windowed deconvolution. The main advantages and the limitation of proposed approach are discussed.

2 Methodology

As previously mentioned, the novel approach takes advantage of the main features of two techniques widely used in seismology and engineering field: the Stockwell Transform (S Transform) and deconvolution interferometry. The main features of the two

techniques are reported briefly in the following paragraphs, and then the combined approach is described.

2.1 Time–frequency analysis: Stockwell Transform

The S Transform (Stockwell et al. 1996) is an invertible time–frequency localization spectral method similar to the short-time Fourier transform (Gabor 1946), but with a Gaussian window whose width scales inversely and whose height scales linearly with frequency (e.g., Parolai 2009; Ditommaso et al. 2012). The S Transform of a function $h(t)$ is defined as

$$S(\tau,f) = \int_{-\infty}^{+\infty} h(t) \frac{|f|}{\sqrt{2\pi}} e^{\frac{-(\tau-t)^2 f^2}{2}} e^{-i2\pi ft} dt \qquad (1)$$

where t is time, f is frequency and τ is a parameter that controls the position of the Gaussian window along the time axis. The S Transform changes the shape of the real and imaginary coefficients over time with the temporal translation of Gaussian window. The 1D function $S(\tau_o, f)$ of variable frequency f for a constant time τ_o, is called the local spectrum.

The important property of S Transform is that it provides a time–frequency representation of local spectrum, with frequency-dependent resolution while, at the same time, it maintains the direct relationship with the Fourier spectrum, $H(f)$, through a simple operation of averaging the local spectra over time (Stockwell et al. 1996) as follows:

$$H(f) = \int_{-\infty}^{+\infty} S(\tau,f) df \qquad (2)$$

Hence, $h(t)$ is exactly recoverable from $S(\tau,f)$. Schimmel and Gallart (2005) showed that, in order to avoid artifacts, the inverse S Transform of the filtered spectra should be carried out by the approximated equation (Simon et al. 2007; Parolai 2009):

$$h(t) = \sqrt{2\pi} \int_{-\infty}^{+\infty} \left(\int_{-\infty}^{+\infty} \frac{S(\tau,f)}{|f|} \right) e^{i2\pi ft} df \qquad (3)$$

Furthermore, thanks to the linearity of the S Transform, it is possible to easily apply a time–frequency filter to the S Transform signal (e.g., Pinnegar and Eaton 2003; Schimmel and Gallart 2005; Parolai 2009) which is especially suitable for extracting the nonlinear dynamic response of structural systems.

2.2 Deconvolution interferometry analysis

Deconvolution interferometry (e.g., Kanai 1965; Snieder and Safak 2006) provides the representation of the dynamic response of a building in terms of a superposition of propagating waves through the structure in the time domain.

An insight about the spatial mass distribution inside the building is obtained, using parameters, like the shear wave velocity, that are connected to the dynamic characteristics of the structure alone, is obtained. The resolution of the retrieve information depends on the number of sensors installed within the building. Assuming a linear and time invariant system, deconvolution interferometry is based on deconvolving the signal $u_{ref}(t)$, recorded

at a reference station at location $\bar{z}$, from the signal $u(t)$ recorded at a generic location z_i. In the frequency domain, the deconvolution can be written as (e.g. Snieder and Safak 2006):

$$D(\omega) = \frac{u(z_i, \omega)}{u_{ref}(\bar{z}, \omega)} \quad (4)$$

in which $u(z_i, \omega)$ and $u_{ref}(\bar{z}, \omega)$ are the Fourier Transforms of the recordings at locations z_i and $\bar{z}$ respectively, and $\omega = 2\pi f$ is the angular frequency.

The choice of the reference station (usually either the roof or the basement of the building) defines different propagating waves through the building and provides complementary information. For a detailed discussion, see Snieder and Safak (2006).

Since this problem is ill-conditioned and hence to avoid the instability, a regularized Tikhonov deconvolution, (Tikhonov and Arsenin 1977; Bertero and Boccacci 1998) is adopted which is defined as

$$D_r(\omega) = F(\omega) \frac{u(zi, \omega)}{u_{ref}(\bar{z}, \omega)} \quad (5)$$

where $F(\omega)$, is the filter, which is defined as:

$$F(\omega) = \frac{\left|u\left(z_{ref}, \omega\right)\right|^2}{\left|u\left(z_{ref}, \omega\right)\right|^2 + \varepsilon} \quad (6)$$

in which ε is the regularization parameter, defined as a percentage of the average spectral power and controls the degree of the filtering applied to the spectral ratio $D(\omega)$.

By taking the Inverse Fourier Transform of $D_r(\omega)$, defined in Eq.(5), the IRF is obtained in the time domain and represents the response of the building to a virtual pulse applied at the reference station. The direct estimate of the pulse velocity (v) is obtained by measuring the wave travel time of IRF. It is worth to stress that in case of bending motion, the pulse velocity obtained in real buildings is dispersive. Moreover, as suggested by Rahmani et al. (2015), the pulse velocity is a constant, characteristic of the frequency band of the impulse responses. Rahmani et al. (2014) showed that, for a broader frequency band, the pulse velocity approaches from below the high frequency asymptote, which is the shear wave velocity of the beam (typically for buildings, which deform more like shear beam). In this work, the shear wave velocity, v_s, is computed since the analyzed building is assumed to behave as a shear beam, as it will explained in the following.

2.3 A combined approach using the Stockwell Transform and deconvolution interferometry

By exploiting the main features of the two techniques, the proposed approach is based on the application of deconvolution interferometry on the time–frequency analysis carried out by the S Transform. The combined approach provides a useful tool for detecting the nonlinear dynamic behavior of a structure in presence of soil–structure interaction through the time-variation of its stiffness, and consequently, of its fixed-base fundamental vibration frequency, f_1, measured according to the corresponding variation of the shear wave velocity.

The S Transform allows the temporal evolution of the fundamental frequency to be followed, but the soil-building system is considered as a whole. Consequently, the variation in fundamental frequency, provided by the S Transform in the time–frequency

domain, can be associated with different sources of nonlinearity (e.g., nonlinear behavior of the structure, dynamic interaction between the structure and soil). On the other hand, the deconvolution interferometry allows the separation of the building's response from the excitation and the ground coupling and therefore is sensitive to structural damage due to its intrinsic local nature. However, it is also hindered by the limitation of time-invariant assumption.

Combining these two techniques, an equivalent linear approach in each frequency dependent window (the signal is considered to be stationary in each frequency dependent window) is proposed. It can be summarized by the following steps:

1. Following Eq. (1), the S Transform is applied to the total duration of the events recorded at the same position on different floors of the instrumented buildings. The local spectrum, defined as $S(\tau_i, f)$, is obtained
2. Taking advantage of mathematical properties such as linearity and ease of filtering of the S Transform, deconvolution interferometry is applied to the local spectra obtained in step 1. In particular, Eq. (5) is modified as follows:

$$D_{r,i}(\tau_i, \omega) = F(\tau_i, \omega) \frac{S(\tau_i, \omega)}{\bar{S}(\tau_i, \omega)} \qquad (7)$$

in which $S(\tau_i, \omega)$ and $\bar{S}(\tau_i, \omega)$ are the local spectra of the recordings at time τ_i (the centre of Gauss scalable window along the time axis), at a generic and the reference location (in this work, the recordings of sensor located at the top), respectively. The filter $F(, \omega)$ in Eq. (6) is modified as follows:

$$F(\tau_i, \omega) = \frac{|\bar{S}(\tau_i, \omega)|^2}{|\bar{S}(\tau_i, \omega)|^2 + \varepsilon_i} \qquad (8)$$

in which $\bar{S}(\tau_i, \omega)$ is the local spectrum at the reference station and the regularization parameter ε_i is defined as percentage of the average local spectral power
3. By taking the inverse Fourier transform of Eq. (7), the instantaneous impulse response functions (IIRFs) are computed at each data point of the seismic event.
4. By measuring the instantaneous time-lag (t_w) as an average of the instantaneous arrival travel time of up-going and down-going waves of the IIRFs, the instantaneous shear wave velocity, $v_s(\tau)$, through the building, is computed over time. In particular, in the presence of a uniform distribution of mass and stiffness along the height of the building, the average v_s inside the building with height H is given by $v_s(\tau) = H/t_w$. If the mass and stiffness of the stories vary, a horizontally layered model can be used and the $v_s(\tau)$ is obtained as a weighted average of the arrival times at the different layers.
5. The variation in time of v_s during a seismic event is compared to its initial value, supposed to be associated to the undamaged structure.

Since v_s depends only on the structural properties and it is not sensitive to the SSI effects (e.g. Snieder and Safak 2006; Todorovska 2009a; Nakata et al. 2013; Rahmani et al. 2014; Ebrahimian et al. 2014), its variations during an event will reflect changes in the structural properties only. In particular, the reduction of v_s during a seismic event is directly related to the degradation of the building's structural stiffness. Hence, v_s is considered to be a damage-sensitive parameter that can be used to detect the onset of the possible structural changes as a consequence of nonlinear dynamic response.

Once v_s is computed, it can be related to the fixed-base fundamental vibration frequency of the structure, f_1, through an analytical relationship depending on the structural type.

Assuming buildings behave as purely shear beams, (e.g. for moment frame structures with rigid floor diaphragms) the fixed-base frequency, f_1, can be estimated from v_s, by using the linear relationship (e.g. Trifunac et al. 2008),

$$f_1 = v_s/4H \tag{9}$$

However, a building can deform as a combination of flexural and shearing deflections and hence, in this case a Timoshenko beam (Timoshenko 1937) model may better approximate its dynamic linear elastic response (e.g. Boutin et al. 2005; Ebrahimian and Todorovska 2014, 2015). In this case, relationships different from (9) should be used for the evaluation of f_1 (e.g. Miranda and Taghavi 2005; Cheng and Heaton 2015; Petrovic et al. 2017a; Michel and Guéguen 2017).

In the following, since the considered building might be reasonably represented as mainly dominated by a shear beam behavior, Eq. (9) will be used for the estimation of the fixed base frequency f_1. Note that we are not mainly focusing on the absolute value but on the relative variation of f_1.

3 The test site: Jalapa Building, Mexico City

The Jalapa building is a 14-story reinforced concrete building which was constructed in 1981 and is located in the central area of Mexico City. It is one of few well-instrumented buildings in Mexico City that has been damaged by several earthquakes and retrofitted twice during its lifetime (e.g. Murià-Vila et al. 2001). The building is 39.5 m high with a rectangular footprint: 19.4 m × 39.70 m from the basement to the 3rd floor, and 19.4 m × 32.00 m in plan from the 3rd floor to the top. There is a 3.3 m deep basement level below the ground. The building is occupied by offices, except for the first three stories which are used as parking. Originally, the structural system consisted of a waffle flat-plate (450 mm thick) on slender rectangular columns with a small core of concrete shear walls around the shaft for staircases and elevator, and with masonry infill walls in the external frames in the longitudinal direction and around the staircases (e.g. Meli et al. 1998).

The soil profile is characterized by a superficial crust about 5 m thick, the upper soft clay deposits extend to a depth of 29.5 m, followed by a 3 m thick intermediate firm layer. A lower clay layer (from 32.5 to 38.5 m depth) overlies deep firm deposits. The average shear wave velocity, estimated through two static cone penetration tests, is equal to about 70 m/s. It is observed that, from the standpoint of mechanical properties, the Mexico City clay exhibits a linear dependence between stress and strain over a large strain amplitude interval, as well as a reduced internal damping ratio (Ordaz and Faccioli 1994). Due to the geotechnical properties of soil and the structural characteristics of the Jalapa building, the dynamic response was influenced by the soil-foundation contribution, as shown by Paolucci (1993), Meli et al. (1998) and Murià-Vila et al. (2001).

The dynamic response of Jalapa building and its interaction with the soil was studied extensively in the past through the Fourier analysis (e.g. Paolucci 1993; Meli et al. 1998; Cardenas et al. 2000; Murià-Vila et al. 2001) and recently by Petrovic et al. (2017b) using the joint deconvolution approach (Petrovic and Parolai 2016). Moreover, Jalapa building suffered structural and nonstructural damage during various seismic events, starting from the 1985 Mexico earthquake. A first attempt to detect the nonlinear seismic response of Jalapa was carried out by Meli et al. (1998) through a modal technique (Li and Mau 1991). Since the entire soil-building system was considered, it was difficult to assess the impact of

the foundation-soil interface. Subsequently, Murià-Vila et al. (2001, 2004) analyzed the changes in the structural characteristics for the four most intense events which occurred during the 1993–1999 instrumentation period. They performed the analyses by the modal technique (Li and Mau 1991) and with a simplified method (Luco 1980) applied on moving windows The variations of the structural parameters have been computed in few disjoint time windows of fixed width.

Figure 1a illustrates the main steps of the life of the building, referring to its seismic response. The 1985 earthquake caused cracks in the columns and in the masonry infill walls and consequently, in 1986, the building was strengthened by the insertion of a shear wall in longitudinal direction and by increasing the sections of column (Paolucci 1993; Meli et al. 1998). During the 1994 earthquake, moderate nonstructural and light structural damage occurred. During the 1995 earthquake, additional structural damage was observed in the walls and columns (e.g. Murià-Vila et al. 2001). Due to the poor structural performance of the original retrofitting, it was upgraded again between 1996 and 1997. The lateral resistance in the transverse direction was strengthened through a continuous X-bracing system across two stories, most of cracks in the columns were repaired with resin and the most damaged masonry walls were replaced. However, the structural performance of the building during the two earthquake events in 1999 with similar peak ground acceleration to some moderate-size earthquakes previously recorded, showed the ineffectiveness of the second retrofitting.

(a)

(b)
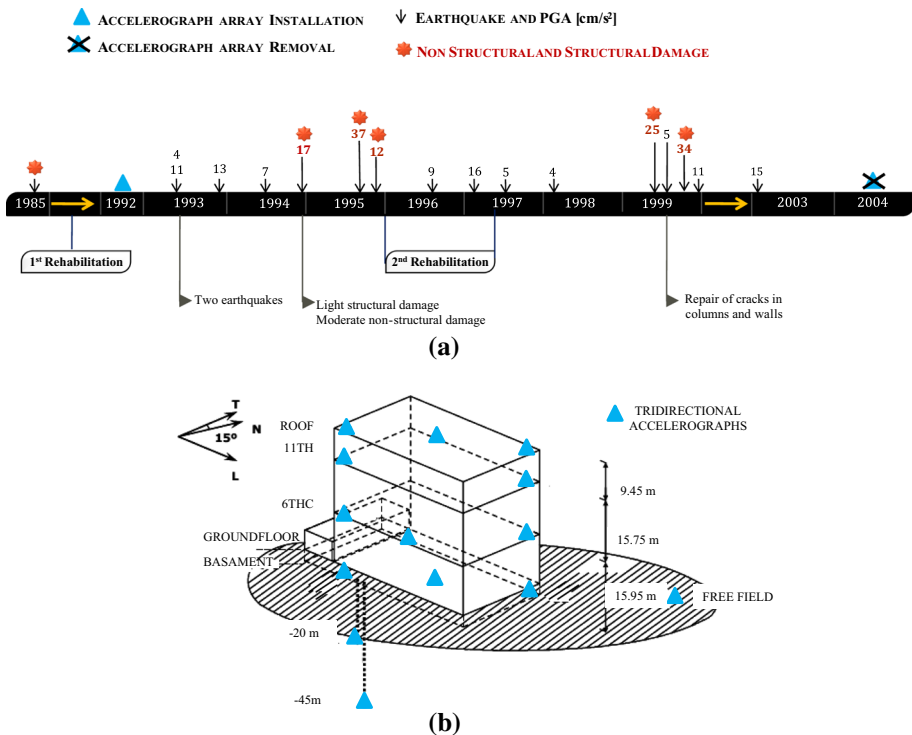
Fig. 1 **a** Timeline of the earthquakes recorded by the sensor location array in Jalapa building from 1992 to 2004. The maximum PGA in cm/s^2 is also reported for sixteen earthquakes, **b** Location and orientation of the building's instrumentation

3.1 Data set

The Jalapa building was instrumented in late 1992 by a 14-accelerograph network (Fig. 1b, blue triangles). The network consisted of two borehole instruments located at 20 and 45 m depth underneath the basement, one instrument at a free-field site (about 50 m away from the building) and eleven instruments at different locations within the structure (basement, 6th and 11th floors, roof). All instruments were 3-component solid state, digital accelerographs (Terra Technology DCA-333R). During the installation period (1992–2004), sixteen earthquakes were recorded with different levels of input shaking, whit the PGA varying from 11 to 37 cm/s^2, as shown in the timeline in Fig. 1a. Three earthquakes are selected for our application: two events (93-2 and 95 in Table 1) before retrofitting during which the response of Jalapa building was essentially linear (93-2 in Table 1) and nonlinear (95 in Table 1) respectively, and one event recorded after retrofitting (99-1 in Table 1) during which the dynamic response changed due to damage and retrofitting. The characteristics of the analyzed events are given in Table 1, with magnitudes ranging from M_w 6.1–7.5, epicentral distances of approximately 220–300 km, and peak ground acceleration (PGA) approximately of 10–40 cm/s^2.

Moreover, the response of the building, in terms of maximum accelerations recorded at the roof and the maximum inter-storey drift (IDR), are also given. The IDR is derived by dividing the relative displacements by the vertical distance between instrumented storeys (roof, 11th, 6th and basement) and the maximum value and is reported in Table 1. In this calculation, the contribution of the dynamic soil–structure interaction is not considered since it is assumed that it did not contribute to the structural damage. It is noted that the maximum IDR reaches 0.3–0.4% for the EQ.95 and EQ.99, which lies within the 0.12–0.6% intermediate level of damage, identified by Murià-Vila et al. (2010) by the presence of cracks in structural and non-structural elements; detachment and falling ceilings. This definition is based on studies of the seismic response of four instrumented buildings in Mexico (Murià-Vila 2007), including Jalapa building.

4 Results

In this study, the horizontal component (instruments aligned along the main building axes) of the three earthquakes recorded by the four sensors located in the basement, on the 6th and 11th floors, and the roof at the west side of the building are considered. Before the

Table 1 Characteristics of the analyzed events and their impact on the building

Event ID	Date	Epicentral distance	M_w	PGA (cm/s^2)	Top building acceleration (cm/s^2) L T		Max drift (%) L T		Visible damage
93-2	15/05/1993	315	6.1	11	27	38	0.05	0.08	No
95	14/09/1995	298	7.5	37	130	110	0.30	0.40	Yes
Jalapa was damaged by 94-95 earthquake and retrofitted									
99-1	15/06/1999	222	6.9	25	86	225	0.13	0.32	Yes

application of the proposed approach, the data are first—band-pass Butterworth filtered [0.1–5 Hz] to encompass the most energetic frequency range amplified by the Mexico City soft clay sediments, giving rise to modulated quasi-sinusoidal motion of long duration and low frequencies at the surface (e.g. Meli et al. 1998).

As underlined by Todorovska and Rahmani (2013), the bandwidth of the original signal is critical for the precision of the peak amplitude of the impulse response function in time. The value around 15 Hz was found as trade-off between smooth impulse response function and accuracy in time. However, the frequency band which contains most of the energy is very narrow for the Mexico City test case, with a frequency range between 0.2 and 2 Hz due to the presence of soft clay that acts as a narrow band pass filter.

Following the steps described in Sect. 2.3, the S Transform is applied on the filtered recordings. Then, the deconvolution interferometry is applied on the local spectra obtained by the use of the S Transform. The regularization parameter ε is set to 5% of the average local spectra power. The value of ε is tested to ensure a good compromise between the numerical stability and the resolution for the inverse problem. The filter $F(\tau_i, \omega)$ is defined based on Eq. (8), by considering the reference station at the top. It is worth to underline that in order to avoid the trade-off between time accuracy and frequency accuracy, the resolution of the IIRFs and thus, the accuracy of estimating the time lags can be improved by resampling the recordings before applying the deconvolution interferometry (e.g., Céspedes et al. 1995; Tamim and Ghani 2010). In our case, this is not necessary due to the fact that the variations related to the sampling rate are much smaller than those caused by the nonlinearity, as shown in the following paragraphs.

4.1 Instantaneous impulse response functions for M_w 6.1 1993 earthquake: linear response

Figure 2a, b show the recordings at the basement of the longitudinal component for 93-2 and 95 events, respectively. The black, blue, green and red lines mark instantaneous times for which the IIRF are shown at different floors in Fig. 2c, d (93-2 event, M_w 6.1, Table 1) and e, f (95 event, Table 1) for the longitudinal and transverse directions.

The shaking amplitude of 1993 event was rather small, with PGA equal to 11 cm/s^2 (Fig. 2a) and the Jalapa building responded linearly since no structural damage was observed after this earthquake. The IIRFs are evaluated at each data point of the EQ.93-2 event. For sake of simplicity, Fig. 2c, d shows four instants of time at which IIRFs are extracted (black line: $\tau = 20$ s, blue line: $\tau = 40$ s , green line: $\tau = 60$ s, red line: $\tau = 80$ s). The peaks of the arrival times of *IIRFs* overlap for the EQ.93-2 event for both horizontal directions (Fig. 2c longitudinal, L; 2d transverse, T). The values of the instantaneous time lags (t_w) are evaluated as an average of the instantaneous arrival travel time of up-going and down-going waves at every locations. Table 2 shows the values of t_w at four instants of time of IIRFs of Fig. 2c, d, at the basement and the 6th floor, in both horizontal directions. Please note that the measured t_w values are estimated form the plots of IRFs and are therefore approximate (as also indicated in Todorovska and Trifunac 2008b). The accuracy of reading the arrival times is estimated to be 0.01, equal to sampling rate. The travel times can be estimated more accurately by fitting a model to the data (e.g. Todorovska and Rahmani 2013; Rahmani et al. 2015), but this is beyond the scope of this paper.

As can be seen, t_w does not experience a noticeable change over time in both directions: in L direction, it is approximately equal to 0.29 s at the basement and 0.25 s at the 6th level
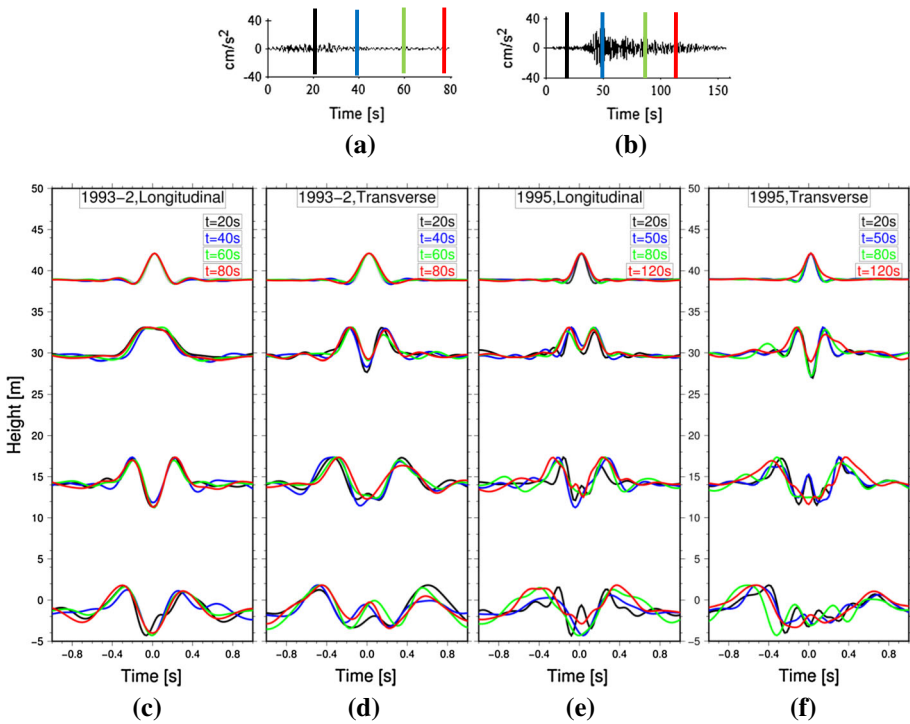
Fig. 2 The 93-2 and 95 earthquakes recorded at the basement are shown in (**a**) and (**b**) respectively, the vertical lines correspond to the time values indicated in the IIRFs plots. Instantaneous impulse response functions (IIRFs) deconvolved with respect to the motion recorded on the roof, during the 93-2 (**c**, **d**) and 95 (**e**, **f**) earthquakes (see Table 3): in the longitudinal (**c**, **e**) and transverse (**d**, **f**) directions. The different colors of lines correspond to different data sampling of recordings (that correspond to the center of the scalable Gaussian window) at which the IIRFs are evaluated

Table 2 Instantaneous time lags t_w at four instants τ of 1993 earthquake duration, at the basement and 6th floor, computed from IIRFs in longitudinal (L Fig. 2a) and in transverse (T Fig. 2b) direction

t_w—Instantaneous time lag (s)

	Longitudinal (L)					Transverse (T)				
τ	20 s	40 s	60 s	80 s	$\Delta\tau$ (%)	20 s	40 s	60 s	80 s	$\Delta\tau$ (%)
Base	0.28	0.28	0.28	0.30	7	0.56	0.55	0.57	0.58	4
6th	0.25	0.25	0.25	0.26	4	0.34	0.33	0.30	0.36	3

The percentage variation of t_w (indicated as $\Delta\tau$) is calculated as the variation of t_w at $\tau = 80$ s with respect to the one at $\tau = 20$ s

over time; in T direction, it is around 0.56 s at the basement level and 0.35 s at the 6th level over time. Comparing the values of t_w evaluated in the L and T direction, a significant difference is detected: the time lag is two times higher in T than in L direction due to different stiffness in both directions. The variation of t_w between $\tau = 20$ s (used as reference value) and $\tau = 80$ s, is computed and indicated as $\Delta\tau$ in Table 2. In both directions,

$\Delta\tau$ is lower than 10% (7% at the basement level, 4% at the 6th level, in L direction; around 4% at basement and 6th floor in T direction).

4.2 Instantaneous impulse response functions for M_w 7.5 1995 earthquake: nonlinear response

The 1995 event (Table 1, ID 95) with magnitude M_w 7.5 was the strongest event that occurred before the retrofitting, with PGA = 37 cm/s^2, four times higher than the PGA of the 93-2 event (Table 1). Due to higher level of shaking (Fig. 2b), significant structural damage was observed. Moreover, Jalapa building was already damaged by the 1994 earthquake when the 1995 earthquake occurred (Fig. 1a).

Figure 2e, f show the IIRFs obtained for the two horizontal components of motion of Jalapa building during the 1995 earthquake The IIRFs are evaluated at each recording sample of the EQ.95 event. As examples, four instants of time are shown in Fig. 2e (longitudinal) and f (transverse), in order to catch the different phases of the event: relatively low amplitudes at the beginning (until $\tau = 40$ s); the intense phase (from $\tau = 50$ s to $\tau = 80$ s) and the ending of shaking motion ($\tau = 120$ s). The meaning of line colors is the same as in the previous case.

Looking at Fig. 2e, f, the IIRFs are characterized by time-shift of the propagating pulses, changing with the shaking level. In the L direction (Fig. 2e), at the basement and 6th floor, the clear increase of the arrival time from the peak of the black line (at $\tau = 20$ s)to consecutive ones (at $\tau = 50, 80, 120$ s) can be observed. The values of t_w (Table 3) experience an increase by 40% from $\tau = 20$ s to $\tau = 120$ s at the basement (from 0.25 to 0.35 s) and 6th floor (from 0.19 to 0.26 s). In T direction (Fig. 2f), the increase of the arrival time is observed at both the basement (by 10% from 0.55 to 0.60 s) and the 6th floor (by 20%, from 0.29 to 0.35 s) when comparing $\tau = 20$ s to $\tau = 120$ s.

4.3 Instantaneous shear wave velocity and the time-evolution of fixed base frequency

The measured t_w between up and down-going waves at different data sample of the recordings is used to evaluate the instantaneous shear wave velocity through Jalapa building. It is worth mentioning that the time-lag between the upgoing and downgoing waves would give only the approximate values for velocities, when the damping is very high (Futterman 1962). It is assumed that this is not the case for the Jalapa building.

Table 3 Instantaneous time lag t_w at four instants τ of 1995 earthquake duration, at the base and 6th floor, computed from IRFs (Fig. 2c, d) in longitudinal (L) and in transverse (T) direction

t_w—Instantaneous time lag (s)

τ	Longitudinal					Transverse				
	20 s	50 s	80 s	120 s	$\Delta\tau$	20 s	50 s	80 s	120 s	$\Delta\tau$
Base	0.25	0.31	0.36	0.35	40	0.55	0.61	0.61	0.60	10
6th	0.19	0.24	0.25	0.26	42	0.29	0.30	0.32	0.35	20

The percentage variation of t_w (indicated as $\Delta\tau$) is calculated as the variation of t_w at $\tau = 120$ s with respect to the one at $\tau = 20$ s

The shear wave velocity changes along the height, from the basement to the 6th floor, and from the 6th floor to the top of the building (Fig. 2) which can be explained by the changes in construction (e.g., changes of inter-story height of the floors used as parking and the others used as offices; changes in dimension of footprint along the height, etc.). Moreover, as reported in Meli et al. (1998), a change in concrete type was detected with height in the building: the average compressive strength was 28 MPa and the modulus of elasticity 19,000 MPa from the basement to the seventh story, and 25 and 18,000 MPa from the seventh story to the top of building. Hence, the building is divided in two layers: one from the basement to the sixth floor and one from the sixth floor to the top of the building (defined by the position where the sensors were installed). The instantaneous shear wave velocity is calculated through a weighted average of t_w of IIRFs at two layers, as follows:

$$v_s(\tau) = \frac{H}{\frac{H1}{V1(\tau)} + \frac{H2}{V2(\tau)}} \tag{10}$$

where $H_1/V_1(\tau)$ is the average time of waves propagating from the basement to the 6th floor (1st layer) and $H_2/V_2(\tau)$ from the 6th floor to the top of building (2nd layer) at the time τ.

Then, the instantaneous values of the fixed-based frequency are computed from the instantaneous shear wave velocities, by assuming that the building behaves as a two layered shear beam. Despite the fact that assuming a building to behave as a pure shear beam is a simplified model, it can be considered a suitable model to reproduce the dynamic behavior of Jalapa building especially before the rehabilitation, since the building floors are considered sufficiently rigid with respect to the columns, in according with the structural model analysis carried out by Meli et al. (1998).

In the following, the instantaneous values of shear wave velocity $v_s(\tau)$ and the corresponding values of fixed-base frequency, $f_1(\tau)$(obtained by $f_1(\tau) = v_s(\tau)/4H$), are evaluated at the four instants of IIRFs of 93 and 95 events. Using the assumption of a building behaving as a shear beam, the values of v_s and f_1 are directly related. For this reason, only the time-trend of f_1 for the analyzed events is shown graphically.

4.3.1 Earthquake 1993: before retrofitting

The instantaneous shear wave velocity $v_s(\tau)$ and the corresponding value of fixed-base frequency, $f_1(\tau)$, are computed from the time lags of the IIRFs of the 93-2 earthquake for longitudinal (L) and transverse (T) directions. The percentage variation of v_s and f_1 with respect to the initial time ($\tau_1 = 20$ s), used as a reference value, is reported in Table 4.

The time-trend of f_1 is presented in Fig. 3, along with the ground shaking at the basement during the 93-2 earthquake in the L (Fig. 3a) and T (Fig. 3b) directions. Despite the fact that the proposed methodology allows the evaluation of f_1 at each data sampling of the shaking motion, for the sake of simplicity, f_1 is evaluated at every 2.5 s of the 93-2 earthquake (black dots in Fig. 3).

It is observed that the $v_s(\tau)$ and hence also $f_1(\tau)$, do not change appreciably in both directions. The variation of these parameters is equal to 5 and 4% from $\tau = 20$ s to $\tau = 80$ s, in L and T direction, respectively (Table 4). In particular, in L direction, the values of $v_s(\tau)$ fluctuate from 124 m/s (at $\tau = 20$ s) to 118 m/s (at $\tau = 80$ s), which corresponds to values of f_1 of 0.75 and 0.72 Hz (Table 4, Fig. 3a). In T direction, the value of

Table 4 Instantaneous shear wave velocity v_s and the corresponding fixed-base frequency f_1 at the four instants τ of the IIRFs (Fig. 2c, d) of 1993 event

	1993—Earthquake										
	τ_1		τ_2			τ_3			τ_4		
	v_s (m/s)	f_1 (Hz)	v_s (m/s)	f_1 (Hz)	Δ (%)	v_s (m/s)	f_1 (Hz)	Δ (%)	v_s (m/s)	f_1 (Hz)	Δ (%)
Long. (L)	124	0.76	124	0.76	–	118	0.72	5	118	0.72	5
Trans. (T)	65	0.40	67	0.40	3	67	0.40	3	63	0.38	4

The percentage of their variations is reported as Δ related to the first value at time τ_1, in longitudinal (L) and in transverse (T) directions

$v_s(\tau)$ varies from 65 m/s (at $\tau = 20$ s) to 63 m/s (at $\tau = 80$ s), which corresponds to values of f_1 of 0.40 and 0.38 Hz, respectively (Table 4, Fig. 3b).

The values of v_s and hence of f_1 obtained by the proposed approach are very low for a RC building of 40 m height, especially in transverse direction, with $v_s = 65$ m/s and $f_1 = 0.40$ Hz. However, these results are in reasonable agreement with the ones reported in literature for Jalapa building. Paolucci (1993) estimated f_1 equal to 0.41 Hz, Murià-Vila et al. (2001) $f_1 = 0.39$ Hz in T direction for 93-2 earthquake. This value reflects the high flexibility in transverse direction of Jalapa building (Murià-Vila et al. 2001). During the second rehabilitation, the building was strengthened by steel bracing which was attached in the central bay of exterior transverse frame through an additional steel and reinforced concrete frame especially in T direction (for details see Murià-Vila et al. 2001). This leads to an increase of fundamental frequency of Jalapa building, as shown for the following event (99-1).
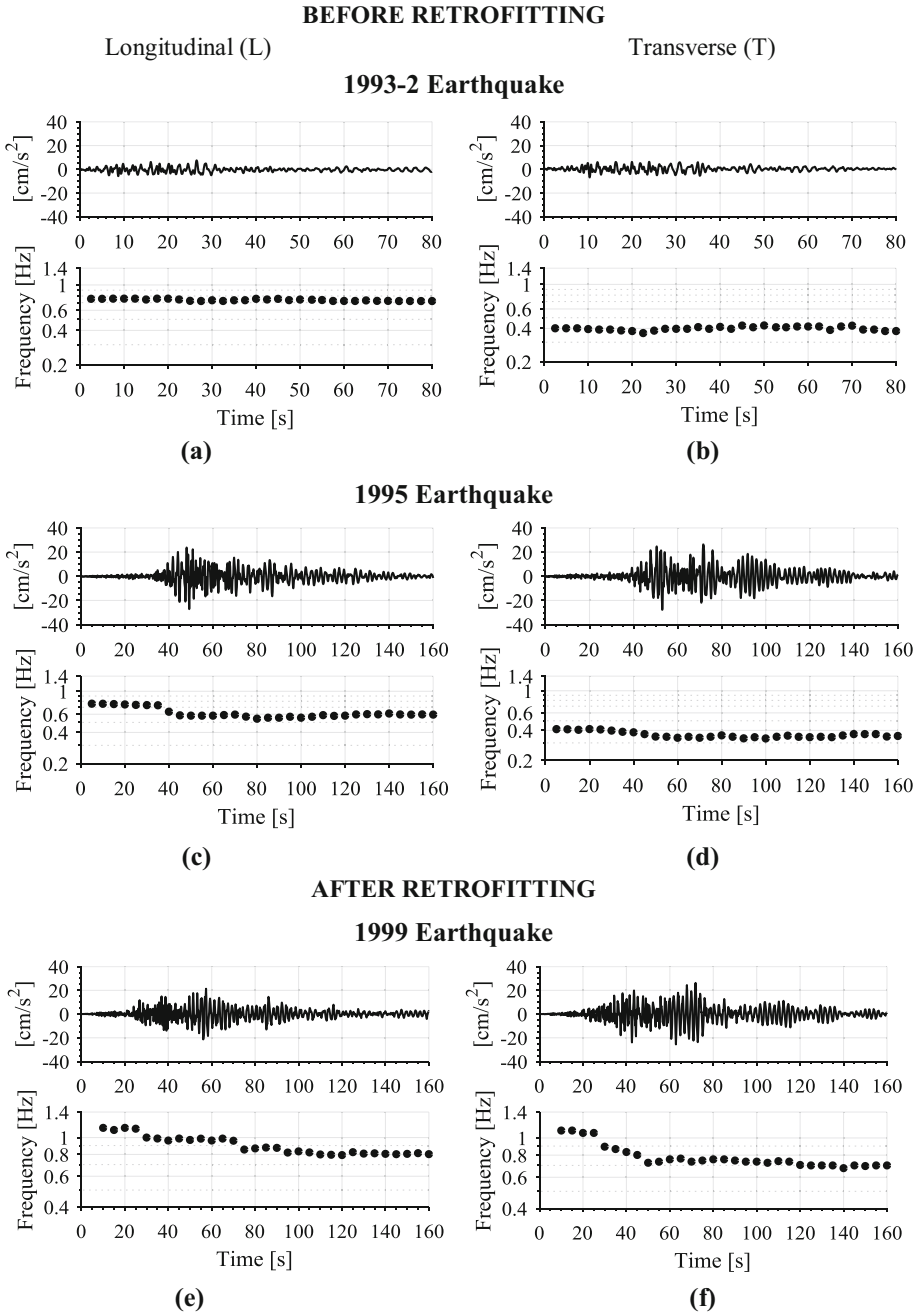
The estimated values of v_s and hence of f_1 have an uncertainty due to the reading errors associated with the picking of the wave arrival time. It is taken into account by considering a reading error of the arrival times equal to $\pm\, 0.01$ (equal to the sampling rate) for the wave arrival time at each location.

The error of estimates results equal on average to $\pm\, 4\%$, in both directions and comparable with the estimated variations of $v_s(\tau)$ and $f_1(\tau)$ during the 93-2. Hence, it is reasonable to conclude that Jalapa building behaved mainly in a linear manner during this event, in accordance with the fact that the small amplitude of the input motion did not cause a considerable change in the dynamic properties of the building.

4.3.2 Earthquake 1995: before retrofitting

The instantaneous shear wave velocity $v_s(\tau)$ and $f_1(\tau)$ are estimated from the four time lags of Fig. 2e, f and reported in Table 5 in both directions for the event that occurred in 1995. Moreover, the time-evolution of f_1 is reported graphically in Fig. 3 in L (Fig. 3c) and in T (Fig. 3d) directions, along with the shaking motion recorded at the basement.

The values reported in Table 5 reveal a reduction of $v_s(\tau)$ and hence, $f_1(\tau)$ during the EQ.95 event. In particular, in the L direction the v_s is estimated to be equal to 125 m/s, and $f_1 = 0.76$ Hz at the smaller amplitude of event (at $\tau = 20$ s), while they drop by 24 and 28% at $\tau = 50$ s and at $\tau = 80$ s, respectively (Table 5). These drops coincide with the strongest phase of shaking (Fig. 3c). When the strong ground shaking ends, a reduction of

BEFORE RETROFITTING

Longitudinal (L)   Transverse (T)

1993-2 Earthquake

(a)   (b)

1995 Earthquake

(c)   (d)

AFTER RETROFITTING

1999 Earthquake

(e)   (f)

Fig. 3 Shaking motion recorded at the basement and time-evolution of fixed-base frequency (f_1) of Jalapa building during three events, before and after the retrofitting. Two events which occurred before retrofitting are shown in longitudinal (L) and in transverse (T) directions: **a**, **b** 1993 earthquake; **c**, **d** 1995 earthquake. One event that occurred after the retrofitting is shown in longitudinal (L) and in transverse (T) direction: **e**, **f** 1999 earthquake. Please note the different horizontal scale that is used for 1993–2 event with respect to other two events and the different vertical scale for 1999 earthquake with respect to 1993 and 1995 earthquakes

Table 5 Instantaneous shear wave velocity v_s and the corresponding fixed-base frequency f_1 at four instants τ of to the IIRFs (Fig. 4e, f) of 1995 event

	1995- Earthquake										
	τ_1		τ_2			τ_3			τ_4		
	v_s (m/s)	f_1 (Hz)	v_s (m/s)	f_1 (Hz)	Δ (%)	v_s (m/s)	f_1 (Hz)	Δ (%)	v_s (m/s)	f_1 (Hz)	Δ (%)
Long. (L)	125	0.76	96	0.58	24	90	0.55	28	94	0.57	25
Trans. (T)	65	0.40	57	0.35	12	58	0.35	10	56	0.34	15

The percentage of their variation is reported as Δ related to the first value at time τ_1, in longitudinal (L) and in transverse (T) directions

25% in the $v_s(\tau)$ and $f_1(\tau)$ remains in L direction, consistent with the occurrence of visible cracks observed in the masonry walls and concrete infill located along the longitudinal direction.

On the other hand, in the T direction, despite the fact that the amplitude of motion at the base is comparable to that in the longitudinal one (PGA $= 37$ cm/s^2), the evolution of v_s and f_1 is characterized by a lower drop over time. The initial v_s is evaluated to be equal 65 m/s, and $f_1 = 0.40$ Hz at the smaller amplitude of event (at $\tau = 20s$), while they decrease by around 10% during the shake motion (Fig. 3d). At the end of the motion, a drop of 15% (Table 5) is observed in $v_s(\tau)$ and $f_1(\tau)$ in T direction (Table 5). The global reduction in velocities and hence in frequencies (25% in L and 15% in T direction) are much larger than the average uncertainties of the estimates, equal to 4%. These estimated reductions are likely due to the structure during the EQ.95, showing nonlinear response, due to the very intense shaking compared to the 1993 event. The higher reduction estimated in L direction is consistent with damage detected in longitudinal masonry infills and concrete infill walls (e.g. Murià-Vila et al. 2001).

4.3.3 Earthquake 1999: after retrofitting

The proposed methodology was also applied to one of the earthquakes recorded in the Jalapa building after retrofitting, with the aim to study the change of dynamic characteristics due to both retrofitting and damage. Despite the fact the Jalapa building was strengthened between 1996 and 1997 (Fig. 1a), structural and non-structural damage was detected after 99-1 event. This earthquake was characterized by peak ground acceleration (25 cm/s^2) similar to that of the 1995 earthquake (34 cm/s^2).

In this section, the main results obtained by the proposed method, namely the time-evolution of f_1 during the shaking, is reported for the 1999 earthquake (Table 1, ID 99-1) and shown in Fig. 3e, d. Note that f_1 is reported at every 5 s of the 1999 event's duration for sake of simplicity.

Our analysis reveals that the structural response deteriorated significantly during the 99-1 earthquake. The decrease in f_1 over time can be observed in both horizontal directions. In L direction (Fig. 3e), the value of f_1 starts from 1.13 Hz at the low amplitude of shaking (until 20 s). A gradually decrease, by 15%, ($f_1 = 0.96$ Hz) can be observed during the intense phase of shaking (from 30 to 70 s) and by 27% ($f_1 = 0.83$ Hz) by the end of shaking (from 30 to 160 s). In T direction, Fig. 3f reveals a rapid drop of f_1, by 35%, (from

1.10 to 0.72 Hz), with the strong input shaking (from 30 to 60 s), ending with the variation of f_1 by 36% ($f_1 = 0.70$ Hz) concurrent with smaller amplitude of the shaking.

Comparing these results to those obtained for the 1995 earthquake, two main differences can be seen: (1) the values of the initial frequencies in both directions are considerably higher than those detected at the end of 1995 earthquake. This is explained by the effects of the retrofitting and the contribution of steel bracing; (2) the Jalapa building behaved in nonlinear manner in both directions, with the estimated permanent variation of f_1 equal to 25 and 35% in L and T direction, respectively, comparable to the variation detected in 1995 in the longitudinal direction. Since the average uncertainty of estimates is about to 5%, these observed variations, which exceeded 20%, are likely to be due to the possible softening related to damage onset.

5 Discussion and conclusion

In this paper, a novel approach is presented to detect the nonlinear dynamic response of damaged structures influenced by soil–structure effects by processing earthquake records and computing the variations of the fixed basefrequencies of the building during a seismic event. In order to monitor the status of a structure during and after earthquakes in presence of soil–structure interaction, it is necessary to decouple the building response from soil–foundation coupling. To this regard, a combined approach of the S Transform and deconvolution interferometry is proposed. It derives from the advantage of the use of the time–frequency representation by application of S Transform to identify the time-variant behavior of the system. Since the variation of the fundamental frequency maybe also related to the nonlinear response at the soil foundation interface, we proposed to apply the deconvolution interferometry to the local spectra of the S Transform because it separates the properties of the building itself from the soil-foundation contributions. Moreover, the limitation to time-invariant system when applying the deconvolution interferometry is overcome in our approach by considering stationarity of the signals in each frequency dependent Gaussian window of S Transform. The main advantage of the proposed method is that provides an estimate of time- variations of the dynamic parameters (such as shear wave velocity and hence the corresponding fixed-base frequency), related only to the occurrence of non-linear response of the structure under a strong earthquake.

The proposed approach is applied to the real data recorded in a reinforced concrete building, the so-called Jalapa building, which suffered structural and non-structural damage, and was retrofitted twice during its lifetime. Soil–structure interaction effects influenced its dynamic behavior due to its location on very soft clay.

The S Transform was selected amongst different time–frequency analyses for the combined method. In order to underline the main features of S Transform, Fig. 4 shows the comparison between different types of time–frequency analyses, including the S Transform. Exemplarily, the time-history acceleration of the 1999 event (ID 99-1, in Table 1), recorded at the top of Jalapa building in longitudinal direction, is considered. Figure 4a shows the Short Fourier Transform (with a Gaussian window); Fig. 4b, c the continuous wavelet transform by varying the types of wavelet: (b) the complex Gaussian wavelet; (c) the complex Morlet wavelet; Fig. 4d the Stockwell Transform. The decrease of the fundamental frequency of Jalapa building can be detected in all representations. It suggests an occurrence of nonlinear behavior of Jalapa building during the 99-1 event, in accordance with the reported damage (Table 1). Nonetheless, there is a main difference between
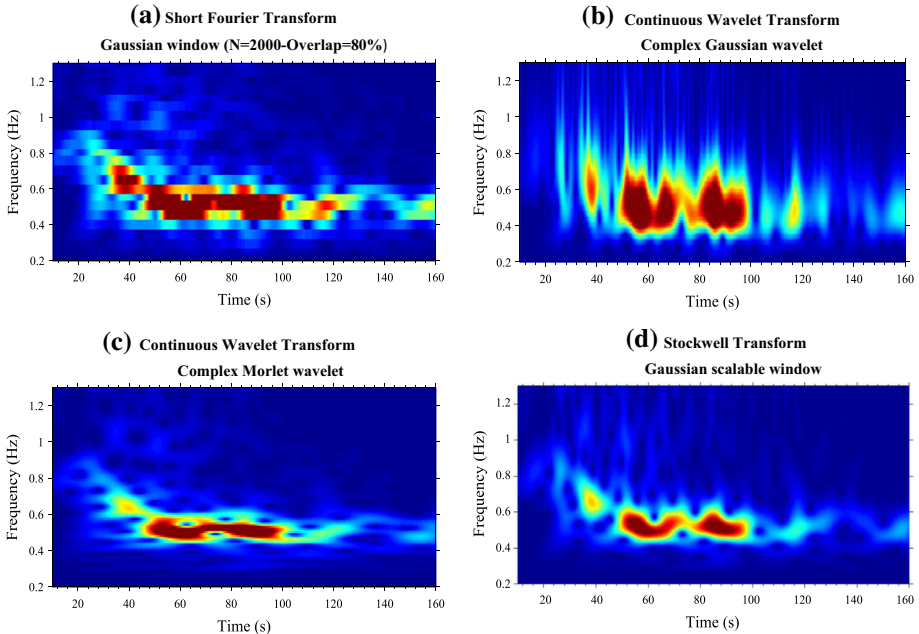
Fig. 4 Time-frequency analysis applied to earthquake-data recorded in Jalapa building during 1999 event (99-1) in L direction. **a** Short Fourier Transform (with Gaussian window); **b**, **c** Continuous wavelet Transform, with Gaussian and Morelet window respectively; **d** Stockwell Transform

the four representations of Fig. 4: the Stockwell Transform (Fig. 4d) provides a better resolution both in time and in frequency domain. Overcoming the difficulties to choose the suitable time-window length for the Short Fourier Transform (Fig. 4b), as well as the type of wavelet in continuous transform (Fig. 4c–d), that depends on the problems that has to investigate. For this reason, the S Transform has been selected for the combined approach.

Three events that occurred in the 1990s in Mexico City and were registered in the Jalapa building are selected in order to investigate the capability of the combined approach of S Transform and deconvolution interferometry to provide reliable results of the evolution of the building properties, consistent with the amplitude of shaking motion and the documented status of the building after each event.

From the analysis of the events that occurred in the period 1993–1995 (before the second retrofitting of the building) and during the 1999 earthquake (after the second retrofitting), it is found that:

- during the smallest event of 1993, the variation of 5% of the v_s and hence, of the f_1 suggests that Jalapa building behaves essentially in a linear manner in both horizontal directions. This result is consistent with the fact that no structural damage was observed after the 1993 earthquake and moreover, the reported maximum inter-storey drift ($< 0.1\%$) was smaller than those commonly associated to the onset of significant structural damage within a reinforced concrete structure.
- during the strongest event of 1995, the dynamic response of the structure is very sensitive to the amplitude of the shaking motion, producing a reduction of 25% of v_s

and hence, of f_1 in the longitudinal direction and of 15% in the transverse direction. The higher variation detected in longitudinal direction is likely due to the amplification effects related to the beatings in the longitudinal direction, well investigated in previous works by Meli et al. (1998) and Murià-Vila et al. (2001). Our results indicate that the dynamic response was nonlinear, which is consistent with the structural damage observed in the longitudinal masonry infills, in the concrete walls and frames, after 1995 earthquake, as well as with the independent estimation of maximum inter-storey drift, that has been higher than 0.3%.

- during the 1999 event that occurred after the second retrofitting, the Jalapa building was also influenced by non-structural linearity, in both directions, with the reduction of f_1 equal to 26 and 35% in L and in T direction, respectively. This is consistent with the high value of inter-storey drift ($> 0.3\%$) and with the evidence that the 1999 earthquake produced severe damage in the building: all masonry walls were damaged, some cracks were opened at the concrete shear walls and in several columns of the main structure, and the deterioration in the interfaces was detected between the new and old structural elements of the transverse facades (Murià-Vila et al. 2001).

Moreover, the time evolution of the fixed-base frequency, obtained by the proposed approach, qualitatively agrees with the previous studies by Murià-Vila et al. (2001). The higher reduction of f_1 was found in the longitudinal direction during the 1995 earthquake and in both horizontal directions during the 1999 earthquake in both analyses. However, a discrepancy of the values of f_1 is observed for EQ.95 and EQ.99. We obtained higher values of f_1, especially during the 1999 earthquake, although the initial values estimated by our approach are in agreement with those obtained from ambient vibration test in 1997 (f_1 is equal to 1 Hz in the L and 0.95 Hz in the T directions), as reported by Murià-Vila et al. (2001). This may be related to different assumptions of the two methods: (1) the deconvolution interferometry provides local estimates, related to the local properties of the structure between the sensors, while Murià-Vila et al. (2001) rely on the modal superposition method that depends on global properties of the structure; (2) our approach is suitable to decouple the structural response from the effects of soil–structure interaction; (3) Jalapa building is assumed to behave as a shear beam. In general, real buildings usually do not behave as pure shear or bending beams, but as a combination of both. Especially after the second rehabilitation, the shear beam assumption might be a too simple one. (4) For a structure behaving as a combination of shear and bending beams, the weight of the two components (shear and bending) is constant, if the building behaves linearly, but will change over time for nonlinear behavior. In future these aspects have to be taken into
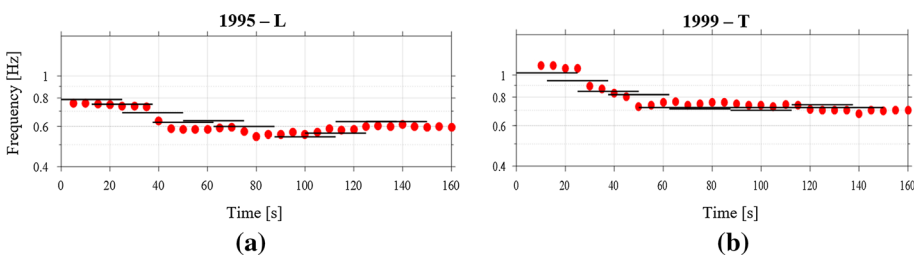
Fig. 5 Comparison between the instantaneous values of the fixed-base frequency obtained by the proposed method (red dots) and those obtained by windowed deconvolution (black lines) by Todorovska and Trifunac (2008a, b). **a** 1995 event—longitudinal direction (L); **b** 1999 event—transverse direction (T)

account in order to be able to improve the estimation of the variation of the fixed-base frequency over time.

Nevertheless, it is worth mentioning that estimating the variation of the shear wave velocity (no assumption on the model describing the building's behavior is needed) in time gives us valuable information about the state of the building and makes it possible to identify if damage occurred. Depending on the number of sensors that has been installed in the building, considering the variation of the velocities through the different layers within the building (defined by the vertical location of the sensors installed within the building), the damage can be not only identified but also localized.

The results in terms of time-evolution of f_1 obtained by the proposed approach are compared with those obtained through the deconvolution interferometry on consecutive time windows during the earthquake shaking (windowed approach), proposed by Todorovska and Trifunac (2008a, b). In order to apply the windowed decovolution, it is necessary to define the length of the time-window and the related overlap. The time-window length can be selected as a function of the fundamental elastic frequency of the structure. If the structure exhibits a nonlinear behavior, the fundamental frequency decrease and it is important to consider this kind of phenomenon by using a moving time-window length greater than length obtained by the elastic fundamental frequency (e.g. Ditommaso and Ponzo 2015). Exemplarily the windowed deconvolution is applied on recordings of 95 and 99 events that caused a high variation of f_1. In particular, the EQ.95 in L direction (with Δf_1 equal to 25%) before the rehabilitation and EQ.99 in T direction (with Δf_1 equal to 35%) after the rehabilitation are selected. In Fig. 5, a comparison between the instantaneous values of f_1 obtained by the proposed method (red dots) and the average values by windowed deconvolution (black line) is shown. For both events, a length equal to 25 s has been used based, following Ditommaso and Ponzo (2015). Moreover, an overlap of 50% of the considered time-window length is chosen. As expected from the documented status of Jalapa building, which suffered severe structural damage during both events, the values of f_1 decrease with time and clear variations of f_1 over time can be detected from Fig. 5.

Overall, the results obtained by the proposed approach and the windowed deconvolution are in agreement. However, there is a main difference between the two approaches and thus the results: the values obtained by the combined approach are instantaneous since they are related to the center of scalable Gaussian window of Stockwell Transform; the values obtained by the windowed deconvolution (2008a) are mean values since they are evaluated in selected windows with fixed width. The proposed approach, based on applying deconvolution interferometry to the local spectra derived using the S Transform, can be considered as a potential tool for detecting the nonlinear behavior associated with structural damage. The estimated variations of f_1 are in reasonable agreement with the documented status of Jalapa building. Thus, the substantial increase of wave travel time, and hence, the decrease in v_s and $f_1 (> 20\%)$ is detected only during earthquakes that caused visible damage This variation can be considered as a global indicator of damage occurrence, since it has been evaluated from motions recorded from four sensors. When more sensors are installed within the structure, the variation of v_s and f_1 will provide a more detailed view of the structural characteristics and hence allow the more localized detection of damage. Further research is needed to determine its effectiveness for detecting degree of damage in buildings, as well as its localization, with a large number of sensors at intermediate floors. In case of lack of dense sensors, Kaya et al. (2015) proposed an accurate

techniques that allow to approximate records at un-instrumented floors from those of the instrumented floors. This issue will be investigated in more detail in the future.

References

Addison PS (2002) The illustrated wavelet transform handbook: introductory theory and applications in science, engineering, medicine and finance. IOP Publishing, Bristol

Askari R, Siahkoohi HR (2007) Ground roll attenuation using the S and x-f-k transforms. Geophys Prospect 55:1–10

Bertero M, Boccacci P (1998) Introduction to inverse problems in imaging. IOP Publishing, Bristol

Bindi D, Petrovic B, Karapetrou S, Manakou M, Boxberger T, Raptakis D, Pitilakis D, Parolai S (2014) Seismic response of an 8-story RC-building from ambient vibration analysis. Bull Earthq Eng 13:2095–2120

Boutin C, Hans S, Ibraim E (2005) Roussillon P (2005) In situ experiments and seismic analysis of existing buildings. Part II: seismic integrity threshold. Earthq Eng Struct Dyn 34:1531–1546

Bradford SC, Yang J, Heaton T (2006) Variations in the dynamic properties of structures: the Wigner–Ville distribution. In: Proceedings of the 8th US national conference on earthquake engineering. San Francisco

Cardenas M, Bard PY, Gueguen, P, Chavez-Garcia FJ (2000) Soil–structure interaction in Mexico City. Wave field radiated away from Jalapa Building: data and modeling. In: Proceedings of 12th world conference on earthquake engineering, Auckland, January 30—Friday 4

Céspedes I, Huang Y, Ophir J, Spratt S (1995) Methods for estimation of subsample time delays of digitized echo signals. Ultrason Imaging 17:142–171

Cheng MH, Heaton TH (2015) Simulating building motion using ratios of the building's natural frequencies and a timoshenko beam model. Earthq Spectra 31(1):403–420

Chopra AK (1996) Modal analysis of linear dynamic systems: physical interpretation. J Struct Eng 122:517–527

Cohen L (1989) Time-frequency distributions—a review. Proc IEEE 77(7):941–981

Daubechies I (1992) Ten lectures on wavelet, Society for Industrial and Applied Mathematics. ISBN 0898712742

Dehghani MJ (2009) Comparison of S-transform and wavelet transform in power quality analysis. World Acad Sci Eng Technol 50:395–398

Ditommaso R, Ponzo FC (2015) Automatic evaluation of the fundamental frequency variations and related damping factor of reinforced concrete framed structures using the Short Time Impulse Response Function (STIRF). Eng Struct 82:104–112

Ditommaso R, Mucciarelli M, Ponzo FC (2012) Analysis of non-stationary structural systems by using a band-variable filter. Bull Earthq Eng 10:895–911

Ebrahimian M, Todorovska MI (2014) Wave propagation in a Timoshenko beam building model. J Eng Mech 140(5):04014018

Ebrahimian M, Todorovska MI (2015) Structural system identification of buildings by a wave method based on a non uniform timoshenko beam model. J Eng Mech 141:1–11

Ebrahimian M, Rahmani M, Todorovska MI (2014) Nonparametric estimation of wave dispersion in high-rise buildings by seismic interferometry. Earthquake Eng Struct Dynam 43:2361–2375

Futterman WI (1962) Dispersive body waves. J Geophys Res 67(13):5279–5291

Gabor D (1946) Theory of communications. J Inst Elect Eng 93:429–457

Ivanovic SS, Trifunac MD, Todorovska MD (2001) On identification of damage in structures via wave travel times. In: Erdik M, Celebi M, Mihailov V, Apaydin N (eds) Strong motion instrumentation for civil engineering structures, NATO Science Series (Series E: Applied Sciences), vol 373. pp 447–467

Kanai K (1965)Some new problems of seismic vibrations of a structure. In: Proceedings of the 3rd world conference on earthquake engineering, Auckland and Wellington, New Zealand

Kaya Y, Kocakaplan S, Şafak E (2015) System identification and model calibration of multi-story buildings through estimation of vibration time histories at non-instrumented floors. Bull Earthq Eng 13(11):3301–3323

Kohler MD, Davis PM, Safak E (2005) Earthquake and ambient vibration monitoring of the steel frame UCLA factor building. Earthq Spectra 21(3):715

Kohler MD, Heaton TH, Bradford SC (2007) Propagating waves in the steel, moment-frame factor building recorded during earthquakes. Bull Seismol Soc Am 97:13341345

Li Y, Mau ST (1991) A case study of Mimo system identification applied to building seismic records. Earthq Eng Struct Dyn 20:1045–1064

Luco JE (1980) Soil–structure interaction and identification of structural models. Proceedings of 2nd ASCE conference on civil engineering and nuclear power, Knoxville, Tennessee; vol 3, no 10, pp 10.1–10.30

Mallat S (1998) A wavelet tour of signal processing. Academic, New York

Meli R, Faccioli E, Murià-Vila D, Quaas R, Paolucci R (1998) A study of site effects and seismic response of an instrumented building in Mexico City. J Earthq Eng 2:89–111

Michel C, Guéguen P (2010) Time–frequency analysis of small frequency variations in civil engineering structures under weak and strong motions using a reassignment method. Struct Health Monit 9(2):159–171

Michel C, Guéguen P (2017) Interpretation of the velocity measured in buildings by seismic interferometry based on Timoshenko beam theory under weak and moderate motion. Soil Dyn Earthq Eng 104:131–142

Michel C, Gueguen P, Lestuzi P (2011) Observed non-linear soil–structure interaction from low amplitude earthquakes and forced-vibration recordings, in Proceedings, 8th international conference on structural Dynamics, EURODYN 2011, Leuven, Belgium, 4–6 July 2011

Miranda E, Taghavi S (2005) Approximate floor acceleration demands in multistory buildings. I: formulation. J Struct Eng 13:203–211

Mucciarelli M, Masi A, Gallipoli MR, Harabaglia P, Vona M, Ponzo F, Dolce M (2004) Analysis of RC building dynamic response and soil-building resonance based on data recorded during a damaging earthquake (Molise, Italy, 2002). Bull Seismol Soc Am 94:1943–1953

Murià-Vila D (2007) Experienciamexicanasobre la respuestasísmica de edificiosinstrumentados, III Coloquio de Ingreso a la Academia. Academía de Ingeniería, México

Murià-Vila D, Rodriguez G, Zapata A, Toro AM (2001) Seismic response of a twice-retrofitted building. ISET J Earthq Technol 38:67–92

Murià-Vila D, Taborda R, Zapata-Escobar A (2004) Soil–structure interaction effects in two instrumented tall buildings. In: 13th world conference on earthquake engineering, Vancouver, BC, August 1–6, paper no. 1911

Murià-Vila D, Aldama BD, Loera S (2010) Structural warning for instrumented buildings. In: Proceedings of the 14th European conference on earthquake engineering, Ohrid, Macedonia, September 2010

Nakata N, Snieder R, Kuroda S, Ito S, Aizawa T, Kunimi T (2013) Monitoring a building using deconvolution interferometry, I: earthquake-data analysis. Bull Seismol Soc Am 103:1662–1678

Nakata N, Tanaka W, Oda Y (2015) Damage detection of a building caused by the 2011 Tohoku-Oki Earthquake with Seismic Interferometry. Bull Seismol Soc Am 105:2411–2419

Ordaz M, Faccioli E (1994) Site response analysis in the Valley of Mexico: selection of input motion and extent of non-linear soil behavior. Earthq Eng Struct Dyn 23:895–908

Paolucci R (1993) Soil–structure interaction effects on an instrumented building in Mexico City. Eur Earthq Eng VII(3):33–44

Parolai S (2009) Denoising of seismograms using the S transform. Bull Seismol Soc Am 99:226–234

Petrovic B, Parolai S (2016) Joint deconvolution of building and downhole strong-motion recordings: evidence for the seismic wavefield being radiated back into the shallow geological layers. Bull Seismol Soc Am 106:1720–1732

Petrovic B, Dikmen SU, Parolai S (2017a) Real data and numerical simulations-based approaches for estimating the dynamic characteristics of a tunnel formwork building. Bull Earthquake Eng. https://doi.org/10.1007/s10518-017-0250-3

Petrovic B, Parolai S, Pianese G, Dikmen SU, Moldobekov B, Orunbaev S, Paolucci R (2017b) Joint deconvolution of building and downhole recordings: an application to three test cases. Bull Earthq Eng (submitted for publication)

Picozzi M, Parolai S, Mucciarelli M, Milkereit C, Bindi D, Ditommaso R, Vona M, Gallipoli MR, Zschau J (2011) Interferometric analysis of strong ground motion for structural health monitoring: the example of the L'Aquila, Italy, seismic sequence of 2009. Bull Seismol Soc Am 101:635–651

Pinnegar CR, Eaton DE (2003) Application of the S-transform to prestack noise attenuation filtering. J Geophys Res 108(B9):2422

Ponzo FC, Ditommaso R, Auletta G, De Muro A (2013) Damage detection on reinforced concrete framed structures using a band-variable filter. Research and applications in structural engineering, Mechanics and computation. In: Proceedings of the 5th international conference on structural engineering, mechanics and computation, SEMC 2013, pp 2303–2307

Prieto GA, Lawrence JF, Chung AI, Kohler MD (2010) Impulse response of civil structures from ambient noise analysis. Bull Seismol Soc Am 100:2322–2328

Puglia R, Ditommaso R, Pacor F, Mucciarelli M, Luzi L, Bianca M (2011) Frequency variation in site as observed from strong motion data of the L'Aquila (2009) seismic sequence. Bull Earthq Eng 9:869–892

Rahmani M, Todorovska MI (2013) 1D system identification of buildings from earthquake response by seismic interferometry with waveform inversion of impulse responses—method and application to Millikan Library. Soil Dyn Earthq Eng 47:157–174

Rahmani M, Ebrahimian M, Todorovska MI (2014) Wave dispersion in high-rise buildings due to soil–structure interaction. Earthq Eng Struct Dyn 44:317–323

Rahmani M, Ebrahimian M, Todorovska MI (2015) Time-wave velocity analysis for early earthquake damage detection in buildings: application to a damaged full-scale RC building. Earthq Eng Struct Dyn 44:619–636

Safak E (1989) Wave propagation formulation of seismic response of multi-story buildings. J Struct Eng ASCE 125(4):426–437

Schimmel M, Gallart J (2005) The inverse S transform with windows of arbitrary and varying shape. IEEE Trans Signal Proc 53:4417–4422

Simon C, Ventosa S, Schimmel M, Heldring A, Dañobeitia JJ, Gallart J, Manuel A (2007) The S-transform and its inverses: side effects of discretizing and filtering. IEEE Trans Signal Process 55:4928–4937

Snieder R, Safak E (2006) Extracting the building response using seismic interferometry: theory and application to the Millikan Library in Pasadena, California. Bull Seismol Soc Am 96:586–598

Stockwell RG, Mansinha L, Lowe RP (1996) Localization of the complex spectrum: the S transform. IEEE Trans Signal Process 44:998–1001

Tamim NSM, Ghani F (2010) Techniques for optimization in time delay estimation from cross correlation function. Int J Eng Technol 10(2):69–75

Tikhonov AN, Arsenin VY (1977) Solution of ill-posed problems. Wiston/Wiley, Washington

Timoshenko S (1937) Vibration problems in engineering, 2nd edn. Van Nostrand, Princeton, NJ

Todorovska MI (2009a) Seismic interferometry of a soil–structure interaction model with coupled horizontal and rocking response. Bull Seismol Soc Am 99:611–625

Todorovska MI (2009b) Soil–structure system identification of Millikan Library North–South response during four earthquakes (1970–2002): what caused the observed wandering of the system frequencies? Bull Seismol Soc Am 99:626–635

Todorovska MI, Rahmani M (2013) System identification of buildings by wave travel time analysis and layered shear beam models—spatial resolution and accuracy. Struct Control Heal Monit 20:686–702

Todorovska MI, Trifunac MD (2007) Earthquake damage detection in the Imperial county services building I: the data and time–frequency analysis. Soil Dyn Earthq Eng 27:564–576

Todorovska MI, Trifunac MD (2008a) Earthquake damage detection in the imperial county services building III: analysis of wave travel times via impulse response function. Soil Dyn Earthq Eng 28:387–404

Todorovska MI, Trifunac MD (2008b) Impulse response analysis of the Van Nuys 7-storey hotel during 11 earthquakes and earthquake damage detection. Struct Control Health Monit 15:90–116

Trifunac MD, Ivanović SS, Todorovska MD (2001) Apparent periods of a building. II: time-frequency analysis. J Struct Eng 127(5):527–537

Trifunac MD, Ivanovic SS, Todorovska MI (2003) Wave propagation in a seven-story reinforced concrete building. Part III: damage detection via changes in wavenumbers. Soil Dyn Earth Eng 23:65–75

Trifunac MD, Todorovska MI, Manić MI, Bulajić B (2008) Variability of the fixed-base and soil–structure system frequencies of a building—the case of Borik-2 building. Structural Control Health Monit 17:120–151

Ville J (1948) Theorieet applications de la notion de signal analytique. Cableset Transm 2A:61

Wen W, Kalkan E (2017) System Identification based on deconvolution and cross correlation: an application to a 20-story Instrumented Building in Anchorage. Alaska, Bull Seismol Soc Am, p 107

Wigner E (1932) On the quantum correction for thermodynamic equilibrium. Phys Rev 40:749–759